TECHNISCHE UNIVERSITÄT
BERGAKADEMIE FREIBERG
The University of Resources. Since 1765.

Max-Planck-Institut
für Biogeochemie

Bachelor Thesis

Tracing large-scale fires from vegetation and soil moisture across different climate regimes

submitted by:

Xinyuan Hou
Matr-Nr. 62078

supervised by:

Priv.-Doz. Dr. Volkmar Dunger, TU Freiberg
Dr. René Orth, Dr. Sungmin O, MPI-BGC

Abstract

Fire is an integral part of the Earth System. Its interactions with the biosphere (vegetation), hydrosphere (moisture) and (emission into) atmosphere have been investigated and are worth further research. In this thesis, the author examined the relationships between fire occurrence and environmental factors using satellite-derived data of burned area, vegetation, soil moisture, and other related weather variables. It is found that fire has the highest frequency under the temperate aridity, which is presumably associated with fuel availability. Climate-dependent, characteristic anomalies of vegetation activity, temperature and soil moisture are potential indicators of future fire occurrence. The study sheds light on the fire-vegetation-hydrology interactions, which might find application in fire forecasting.

Keywords: fire; burned area; climate; vegetation; soil moisture; remote sensing.

Statement of Authorship

The author hereby declares to be the sole author of this bachelor thesis and that she has not used any sources, than those, listed in the references. It has not been accepted in any previous application for a degree.

Acknowledgements

Many thanks to Priv.-Doz. Dr. Volkmar Dunger for accepting as the university reviewer. The work described here was carried out in the research group of Hydrology-Biosphere-Climate Interactions at the Max Planck Institute for Biogeochemistry between April and June 2019. The author wishes to thank Dr. René Orth for suggesting this topic, and for all the valuable supervision he and Dr. Sungmin O provided. Other group members contributed to the progress through regular group meeting discussions. Dr. Roman Andreev took the time to read this thesis and provided enlightening comments. All of them the author gratefully acknowledges here with much sincere appreciation.

Jena, 20.06.2019 Xinyuan Hou

Contents

List of Figures

1 Introduction

In a global perspective, fire is ubiquitous, although its extent and frequency vary across different ecosystems, within which different controlling factors dominate. Fire per se has a spectrum of functionality. For instance, in circumboreal forests, fire serves as a stand-renewing agent and is regarded as ecologically desirable (Flannigan et al., 2009). As part of land management, prescribed fires to prevent wildfire and agricultural fires to facilitate harvest are practiced in many regions (Youssouf et al., 2014). However, fire can also be disastrous. Even for regions where merely a small fraction of the area is burned, the local ecological effects can be substantial and contribute to drastic ecosystem changes over time (Littell et al., 2009). When occurred in populated regions and are fueled by high temperatures and wind speeds, fires cause damage to properties, deteriorate well-being of living creatures; human health is also threatened by trace gases and aerosols emitted by wildfires, the effects of which are by far poorly quantified (Youssouf et al., 2014).

Previous studies have established the determinant effect of weather/climate on fire (Littell et al., 2009; Flannigan et al., 2009). Many of the severest fires are accompanied by extreme weather (Flannigan & Wotton, 2001). Weather influences fire by affecting fuel moisture, lightning, fire grow through wind control (Flannigan et al., 2005; Littell et al., 2009). There is a consensus that the ongoing and anticipated climate change is expected to alter fire activity (frequency, severity) spatially and temporally and to lengthen fire seasons (Turner & Romme, 1994; Flannigan et al., 2009). However, a clear relationship between climate and fire occurrence is not determined in some studies, leaving room for other yet-to-be-identified ignition mechanisms (Moreira et al. 2011).

Besides climate as the primary driver, crucial factors contributing to wildfire include fuel accumulation and fuel moisture content (Jensen et al., 2018). Littell et al. (2009) pointed out that although seasonal to inter-annual climate variation is paid less attention, the extreme weather on a long timescale often affects the burned area through the production and senescence of vegetation (controls on fuel moisture and continuity). Fuel load influences fire intensity and fuel moisture content influences both fire ignition and spread, directly affecting wildfire behavior (Burapapol & Nagasawa, 2016). Wet fast-growing vegetation contributes to fire proliferation and persistence after ignition owing to higher primary production, thus increasing available fuel (Jensen et al. 2018).

Temperature and moisture are critical elements that determine inter-annual variability of burned area (fire spread) (Moreira et al., 2011). Higher air temperatures accelerate plant senescence and promote fire ignition; the humidity regulates the combustion through moisture content available for vegetation (Krueger et al., 2015). Impacts of soil moisture on wildfire have been little investigated, but it is recommended to be incorporated in wildfire

risk assessment as soil moisture is involved in direct physical interactions between soil and plants (Krueger et al., 2015).

Specific analyses of fire in the first half of the twentieth century were hindered by the lack of complete high-resolution burned area data prior to the year 1980 (Littell et al., 2009). With the help of modern remote-sensing of essential climate variables (temperature, land cover, soil moisture, among others), comprehensive studies of elaborate interactions between the atmosphere, hydrosphere and biosphere are made possible. For instance, Forkel et al. (2017) found that under wet conditions and with restriction to vegetation (type, density and biomass), fire activity can be better predicted by global fire models.

The objective of this thesis is to investigate the relationships between fire occurrence and environmental factors using satellite-derived data of burned area (fire), vegetation, soil moisture, and other related weather variables. The following specific questions are to address:

- How are the fire occurrences distributed globally across different climate regimes?
- How do fires, vegetation and soil moisture interact?
- How and to what extent do vegetation and soil moisture contribute to fire occurrences?
- How long do the impacts of fires on vegetation and soil moisture last?

2 Data and methods

2.1 Datasets

From the European Space Agency's Climate Change Initiative (ESA CCI), the datasets of burned area (version 5.1) are retrieved. The products of burned area are based on spectral information from the Moderate Resolution Imaging Spectroradiometer (MODIS) and thermal information from the MODIS active fire products (Chuvieco et al., 2016), which are available monthly from 2001 to 2017 at two resolutions: pixel (approximately 250 meters) and grid (0.25 degree latitude × longitude) (`https://geogra.uah.es/fire_cci/`).

The ESA CCI soil moisture datasets (version 04.4, combined) merged passive and active microwave retrievals from satellite instruments and were rescaled using a land surface model (Liu et al., 2012). The values are daily available and have the unit of volume percent.

The normalized reflectance difference between the near-infrared and visible red bands is termed to be the Normalized Difference Vegetation Index (NDVI), which measures changes in chlorophyll content (Rouse et al., 1974), indicating the greenness or photosynthetic activity of the vegetation. The value is between -1 and 1. The dataset of NDVI comes from the fourth version of the National Oceanic and Atmospheric Administration (NOAA) Climate Data Record of Advanced Very High Resolution Radiometer (AVHRR) Surface Reflectance (Vermote et al., 2014). Its temporal resolution is half-monthly (with values of the 1st and the 15th day of the month).

The temperature, precipitation and radiation data are derived from the ERA5 reanalysis (Hersbach & Dee, 2016) by the European Centre for Medium-Range Weather Forecasts. The data have a daily temporal resolution. The monthly data of temperatures were used in this study.

The employed gridded data are of the global domain and summarized in Table 1.

Table 1: Overview of the considered variables

Variable	Temporal resolution	Spatial resolution	Dataset	Reference
Burned area	Monthly	0.25	ESA MODIS Fire_cci v5.1	Chuvieco et al., 2016
Soil moisture	Daily	0.50	ESA CCI soil moisture v04.4 (combined)	Liu et al., 2012
NDVI	Half-monthly	0.50	NOAA AVHRR	Vermote et al., 2014
Temperature	Monthly	0.25	ERA 5	Hersbach & Dee, 2016
Precipitation	Daily	0.50		
Radiation	Daily	0.50		

2.2 Spatio-temporal aggregation

The analyses were conducted for the period from January 2001 to December 2016. All data used in this study were aggregated to the spatio-temporal resolution of the burned area (BA) data; i.e., 0.5 degree and monthly scales. Datasets with spatial resolution lower than 0.25 degree were downscaled to 0.25° × 0.25° by repeating the value of each grid cell once along the longitude and once more along the latitude.

The monthly burned areas were summed over the 16 years to produce a global map. The monthly temperatures were averaged over the 16 years to obtain the long-term mean temperature. The net radiation is the daily summation of surface net solar radiation and surface net thermal radiation in the original dataset (C3S, 2017). Next, precipitation and net radiation were summed over 365 or 366 timesteps within the single year before the ensemble mean of each was computed over the 16 years. These datasets were processed using the Climate Data Operator (Schulzweida, 2019).

For soil moisture (SM), only grid cells with at least eight available daily values every month were used for the monthly mean calculation. Other grid cells were regarded as a lack of reliable data and set blank. The average of the two NDVI values every month was set as the monthly mean. Only grid cells with burned area > 0 and a fraction of observed area ≥ 80 % were considered.

2.3 Climate regimes

To construct the distribution of fire occurrence, one needs to define specific climate regimes with specified mean temperature and aridity. The aridity index (AI) after Budyko (1974) was obtained using the following formula:

$$AI = \frac{\frac{R_{net}}{f}}{P} \tag{1}$$

AI: aridity index, dimensionless

R_{net}: long-term average of annual net radiation in MJm^{-2}

f: conversion factor of radiation to equivalent evaporation, f = 2.45 (Allen et al., 1998)

P: long-term average of annual precipitation in mm

Taking into account the physical conditions of fire events, one chose temperatures ranging from 0 to 30 °C with an interval of 5 °C and aridity index from 0.25 to 16 with a logarithmic scale of base two. The numbers of grid cells with burned area sum > 0 for every climate regime were computed. As this approach does not include the frequency of fire events (one grid cell can have several fires during the 16 years, it is nevertheless counted once), another approach to include the temporal factor was applied: in each climate regime, the burned ratio (BR) was computed using the following formula:

$$BR = \frac{\sum_i m_i}{N_{\text{total}} \times 16 \times 12} \times 100\% \tag{2}$$

BR: burned ratio, %

m_i: number of months over the 16 years with nonzero burned area in grid cell i

N_{total}: number of grid cells within each climate regime

In this way, the hotspot was selected as a reference to analyze pre-/post-fire vegetation and soil moisture behaviors across different climate regimes.

2.4 Temporal evolution

Within each climate regime, the year and month of the maximum burned area over the 16 years in every grid cell were chosen (thus large-scale fires in terms of the single grid cell). For the pre-/post-fire comparison, one calculated the anomalies of NDVI, soil moisture and temperature over eight months before and after the month with the maximum burned area, excluding the fire events in the first eight months of 2001 and the last eight months of 2016. The original time series of the values subtracted by their 16-year seasonal average are the anomalies. To minimize the effect of outliers, median burned area, anomalies of NDVI, soil moisture and temperature of each regime were selected.

3 Results

3.1 Fire distribution

The fire data from ESA CCI deliver an annual global burned area of 4.66 million square kilometers between 2001 and 2016. Using the fourth generation of the Global Fire Emissions Database (GFED4) gives an estimate of 3.48 million square kilometers (1997-2011) of global annual burned area (Giglio et al., 2013). Figure 1 is a global map of the cumulative burned area between 2001 and 2016. The most burned area is observed in Africa (south of Sahara), South America (the majority in Amazon Basin) and Northwestern Australia. Significant fire activity is also found over Eastern Europe and Western Asia. Some scattered fires are observed in North America and Northern Asia (mainly Siberia). It is noticeable that the cumulated burned area in some islands and archipelagos (e.g., the Malay Archipelago) is also visible from the map.

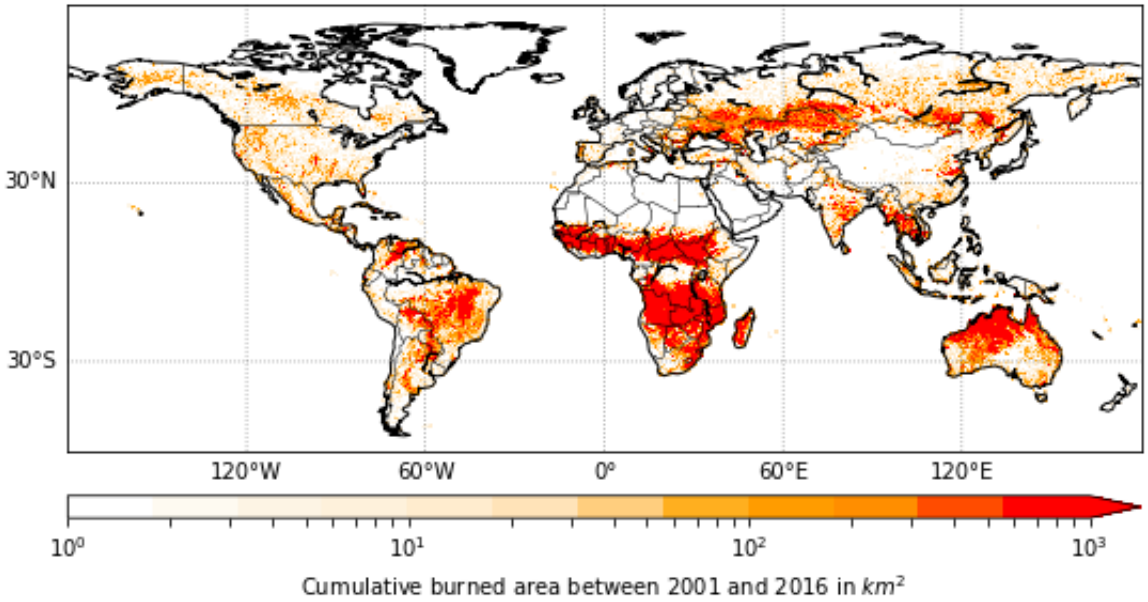

Figure 1: Global map of the cumulative burned area between 2001 and 2016. The logarithmic scale is used to level the non-normal distribution.

The information of the cumulative burned area was remapped onto the two-dimensional space to identify fire regimes in terms of temperature and aridity. Figure 2 (left) shows the number of grid cells with burned area >0 during the study period. There are more grid cells with fire in regimes of AI ranging from 0.5 to 4 than in other aridity ranges. In arid regimes (AI>4), one can observe more grid cells with nonzero burned area where the temperature is higher than 15 °C. Comparatively fewer grid cells have area burned in them where are very humid or arid (AI smaller than 0.5 or larger than 8). Fire hotspots appear in the regimes of temperature 20 to 30 °C and aridity index of 1 to 2. The regime with the lowest temperatures (0-5 °C) also has a high quantity of grid cells with fire occurrence. For

data effectiveness, the regimes with burned grid cell numbers lower than 100 would not be considered for later analyses of pre-fire anomalies as well as post-fire recovery.

Figure 2 (right) represents the pre-defined Burn Ratio (i.e., frequency of fire occurrence) across different climate regimes. The grid cells in the regimes with AI between 1 to 4 have overall higher BRs than those in the regimes with lower or higher AI. The regimes with lower AI but temperatures higher than 20 °C also exhibit relatively high BRs. Fire has the highest frequencies in the temperature range of 20 to 25 °C and the AI range of 1 to 2. The second largest BR occurs in the climate regime with the temperature range of 0 to 5 °C under the same aridity. In general, aridity plays a more critical role in determining fire regimes than temperature does.

While the count of grid cells with burned area mainly focuses on one spatial aspect of fire occurrence, the BR takes into account the number of grid cells that belong to the same climate regime regardless of fire occurrence. Therefore, the temperature and aridity range of the bin with the highest BR (T 20-25 °C and AI 1-2) were chosen as the reference because of the higher representativeness. Three regimes in the same temperature range as the reference (20-25 °C) and three in the same AI range as the reference (1-2) were selected for further analyses.

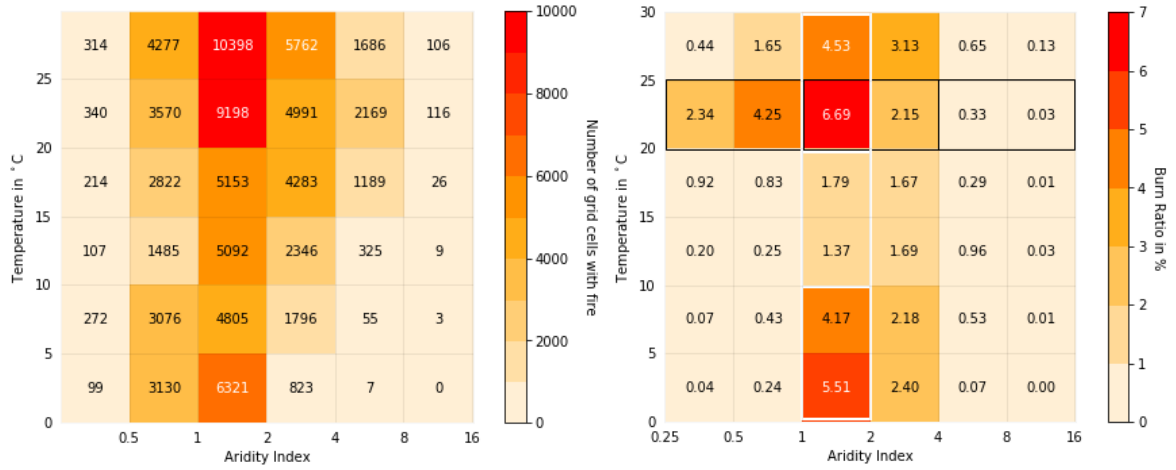

Figure 2: Fire distribution across different climate regimes. Left: Number of grid cells with burned area >0; right: Burn Ratio in percentage. Black and white boxes represent the three selected regimes of the reference temperature range (20-25 °C) and AI range (1-2), respectively.

3.2 Temporal evolution

Figure 3 shows the median burned area (in km^2) for each pre-defined regimes. In the temperature range of 20 to 25 °C (Figure 3, upper), the median burned area per grid cell in the wet regime (AI 0.25-1) is smaller than that in more arid regimes (around 15 km^2). The moderate (AI 1-4) and arid (AI 4-16) regimes show very similar maxima of median burned area per grid cell (approximately 53 km^2), as the peaks are rarely visually distinguishable.

In the moderate regime, the month before and after the month with the peak burned area have larger burned area than that in the arid regime, possibly indicating different fire characteristics (e.g., fire persistence). At the reference temperature range, a wetter condition signifies a smaller burned area.

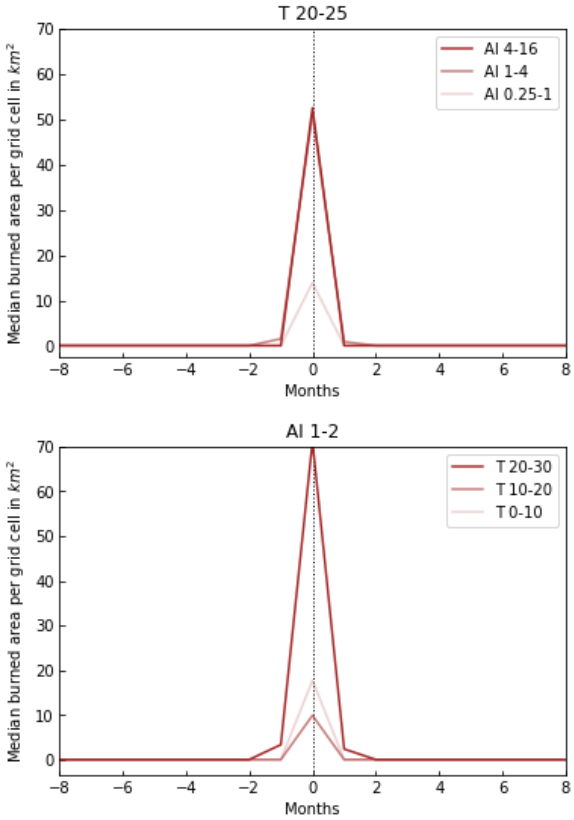

Figure 3: Temporal evolution of median burned area per grid cell (from eight months before to eight months after the month with the peak burned area). Upper: regimes at the reference temperature range with different aridity ranges; lower: regimes at the reference aridity range with different temperature ranges.

In the AI range of 1 to 2 (Figure 3, lower), the largest median burned area per grid cell occurs in the hot regime (T 20-30 °C), followed by the cold regime (T 0-10 °C) with a median burned area less than 20 km^2. The moderate regime (T 10-20 °C) have relatively smaller median burned area per grid cell (slightly > 10 km^2). For this aridity range, there are more burned areas in regions with high and low temperatures than in temperate regions.

Figure 4 shows the temporal evolution of the median NDVI anomaly before and after the month with the peak burned area. In the temperature range of 20 to 25 °C, NDVI experiences a positive anomaly until around one or two months before the month with the peak burned area in the three presented regimes (Figure 4, upper). Then NDVI drops to an under-average level with the onset of fire. Several months before the fire, NDVI in the arid regime (AI 4-16) have the highest median positive anomalies; after the fire, it even further decreases until the crest four months after the month with the peak burned area.

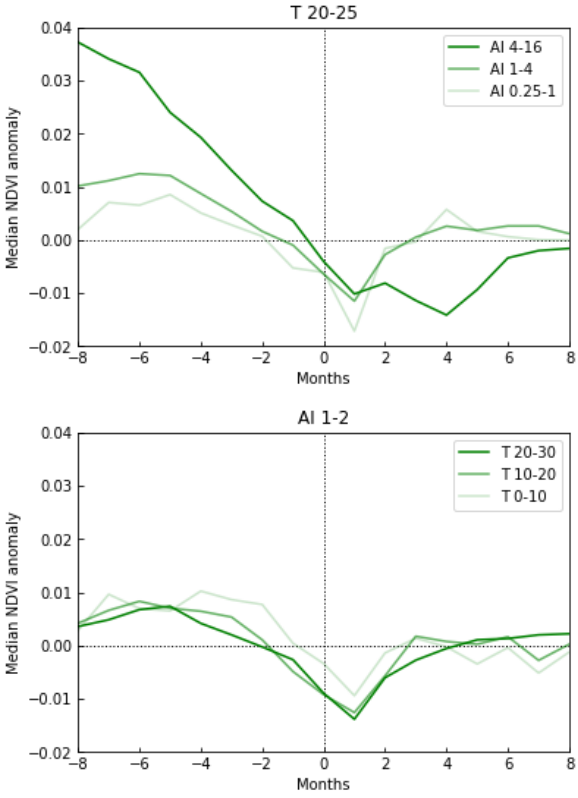

Figure 4: Temporal evolution of median NDVI anomaly (from eight months before to eight months after the month with the peak burned area). Upper: regimes at the reference temperature range with different aridity ranges; lower: regimes at the reference aridity range with different temperature ranges.

Under the same aridity (AI 1-2) (Figure 4, lower), in the moderate (T 10-20 °C) and hot (T 20-30 °C) regimes, NDVI exhibits a similar development as in the upper figure, with negative anomalies in the hot and moderate regimes larger than that in the cold one.

Figure 5 shows the temporal evolution of median temperature anomaly before and after the month with the peak burned area. Across all six selected regimes, temperature anomalies turn positive from negative before the month with the peak burned area.

In the temperature range of 20 to 25 °C (Figure 5, upper), regimes of all three aridity ranges witness the highest positive temperature anomalies at the month with the peak burned area. The arid regime (AI 4-16) exhibits the most significant fluctuation of anomalies, whose median reaches a deviation of nearly one degree Celsius. In the aridity range of 1 to 2 (Figure 5, lower), the most substantial fluctuation of median temperature anomalies occurs in the cold regime (T 0-10 °C). However, negative anomalies of temperature are more trivial than their positive counterparts.

Figure 6 shows the temporal evolution of median soil moisture anomaly before and after the month with the peak burned area. Under the same observed temperature (T 20-25 °C), the soil moisture anomalies turn negative from positive around one to three months

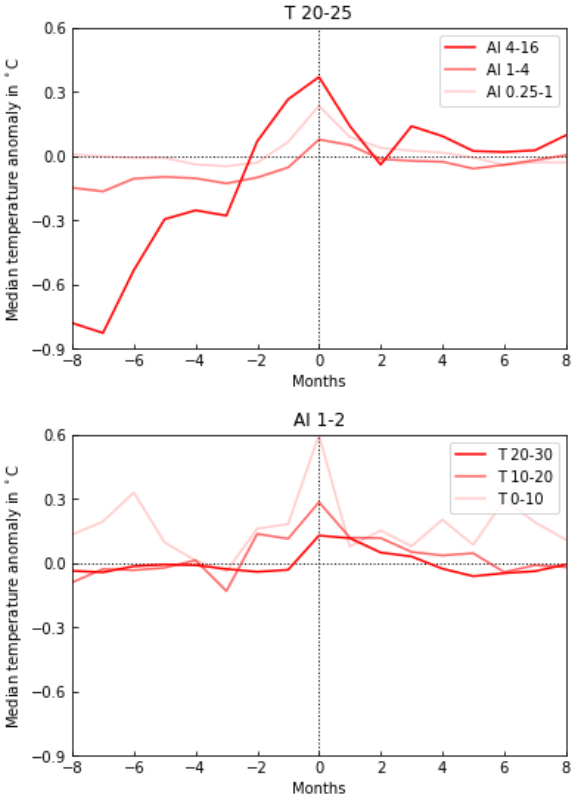

Figure 5: Temporal evolution of median temperature anomaly (from eight months before to eight months after the month with the peak burned area). Upper: regimes at the reference temperature range with different aridity ranges; lower: regimes at the reference aridity range with different temperature ranges.

before the month with the peak burned area (Figure 6, upper), except for the wet regime (AI 0.25-1), whose median pre-fire anomalies are always negative. In the arid regime (AI 4-16), the curve appears extraordinarily spiky; the median anomaly even turns less negative during the two months around the month with the peak burned area before plummeting to the trough four months after the month with the peak burned area.

Under the same investigated aridity (AI 1-2), soil moisture experiences a positive anomaly several months before the month with the peak burned area; then it decreases to the trough during the fire or with a one-month time lag. After at least four months, it recovers to the normal status. The median positive anomalies are generally smaller than negative ones.

Note that the trends of NDVI and soil moisture development merely represent median behaviors and do not apply to every single fire event. As can be observed from the 5th-95th percentile of the ensemble median of NDVI as well as SM anomaly in the regime with the temperature range of 20-25 °C and AI range of 1 to 4 (Figure 7), even when the median value indicates a positive or negative anomaly, there are accordingly negative or positive anomalies in the data series.

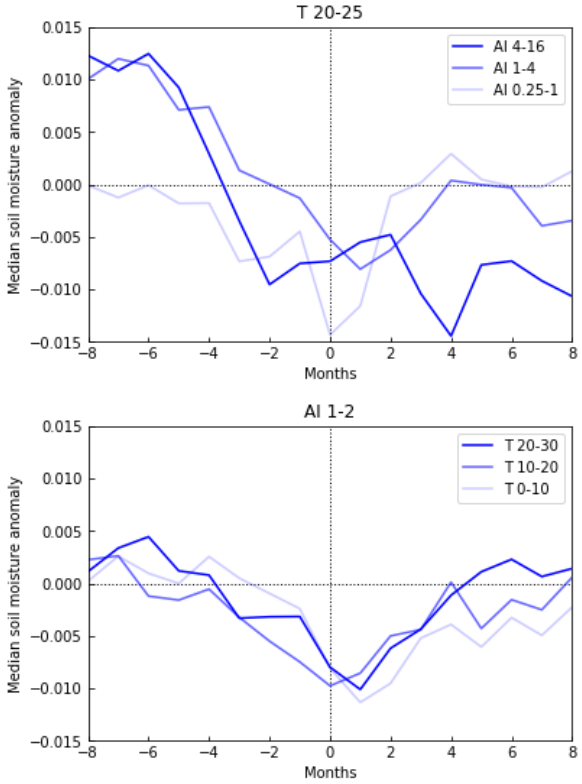

Figure 6: Temporal evolution of median soil moisture anomaly (from eight months before to eight months after the month with the peak burned area). Upper: regimes at the reference temperature range with different aridity ranges; lower: regimes at the reference aridity range with different temperature ranges.

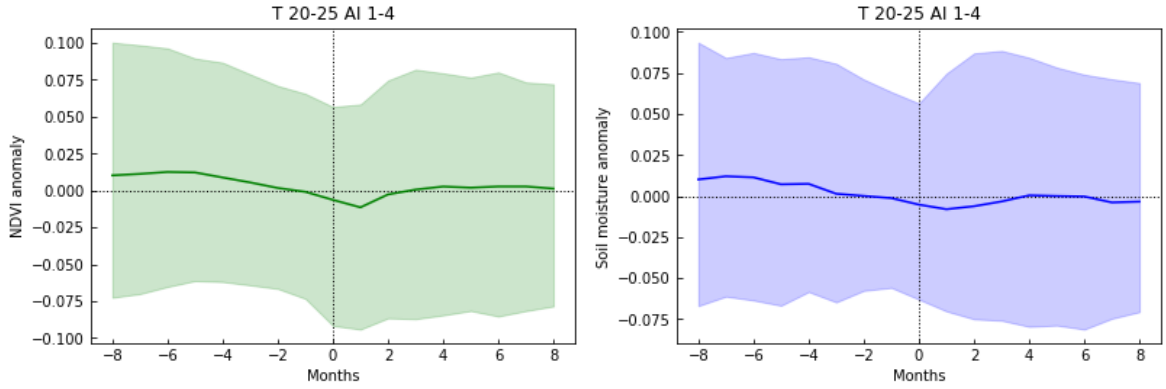

Figure 7: Temporal evolution of anomalies in the regime with the temperature 20 to 25 °C and AI range of 1 to 4. The solid lines show the median anomalies, while the color shades denote the 5th-95th percentile of the median anomalies. Left: NDVI; right: soil moisture.

3.3 Pre-fire anomaly

Pre-fire vegetation, temperature and soil moisture behaviors over the entire climate regimes are further investigated in this section. Figure 8 shows the median NDVI anomaly for each climate regime. Four months before the month with the peak burned area (Figure 8, left), most of the regimes with valid data exhibit positive median NDVI anomalies, except for two regimes in the high-temperature range. Although a convincing distribution of NDVI anomaly lacks, the vegetation has generally higher activity than its long-term average (pos-

itive NDVI anomaly) four months before the fire, with the hotspots in the regimes of AI 2 to 8.

As two more months elapse (Figure 8, right), no universal development of median NDVI anomaly can be confirmed. Eight of the 29 observed regimes see an increase of NDVI anomaly to various extent, the rest witness decreases. Despite this spatially heterogeneous pattern, most of them remain positive.

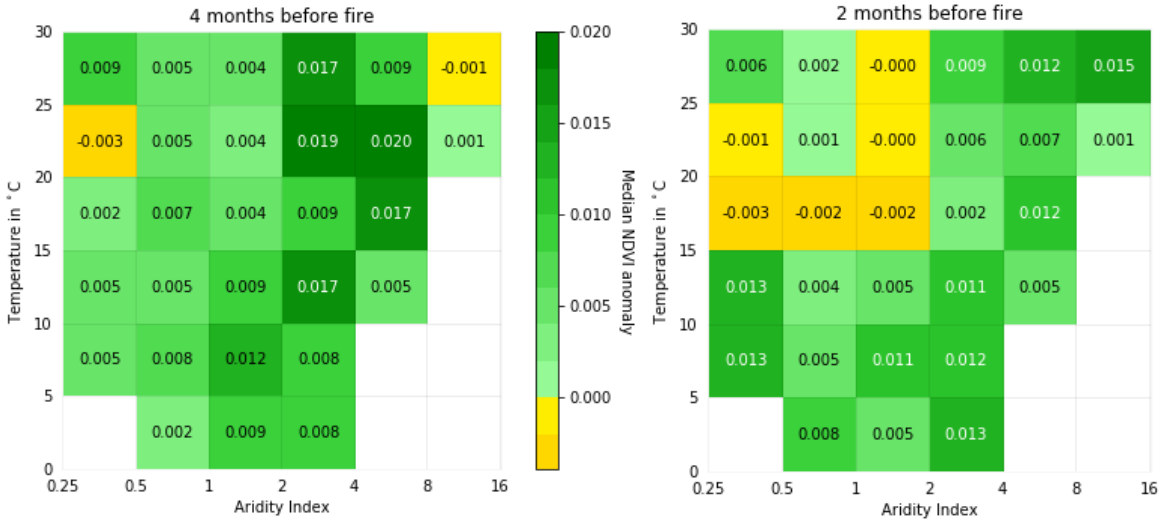

Figure 8: Median NDVI anomaly of each regime. Left: four months before the month with the peak burned area; right: two months before the month with the peak burned area. The two heatmaps share the same color bar. Empty bins denote that the regime is left out due to its low number of grid cells with valid data (<100).

Figure 9 shows the median temperature anomaly for each climate regime. Around half of the regimes (15 in 29) have negative median temperature anomalies four months before the month with the peak burned area (Figure 9, left). Two months later (Figure 9, right), however, more positive anomalies emerge in the regimes at the lower left locations along the diagonal from the upper left to the lower right. In the hotspots of fire occurrence, most temperature anomalies remain negative.

Figure 10 shows the median soil moisture anomaly for each climate regime. Four months before the fire event (Figure 10, left), more than half of the regimes exhibit positive soil moisture anomalies. In the regimes of high temperatures (T > 20 °C) and high aridity (AI > 1), the anomalies are generally higher than in other regimes. They are also regimes showing high numbers of grid cells with nonzero burned area and high BRs.

When time goes to two months before the fire (Figure 10, right), there are more regimes with negative soil moisture anomalies than positive ones. For those with still positive anomalies, almost all of them experience a decrease in soil moisture after two months. There are only three regimes whose anomalies increase in the meantime.

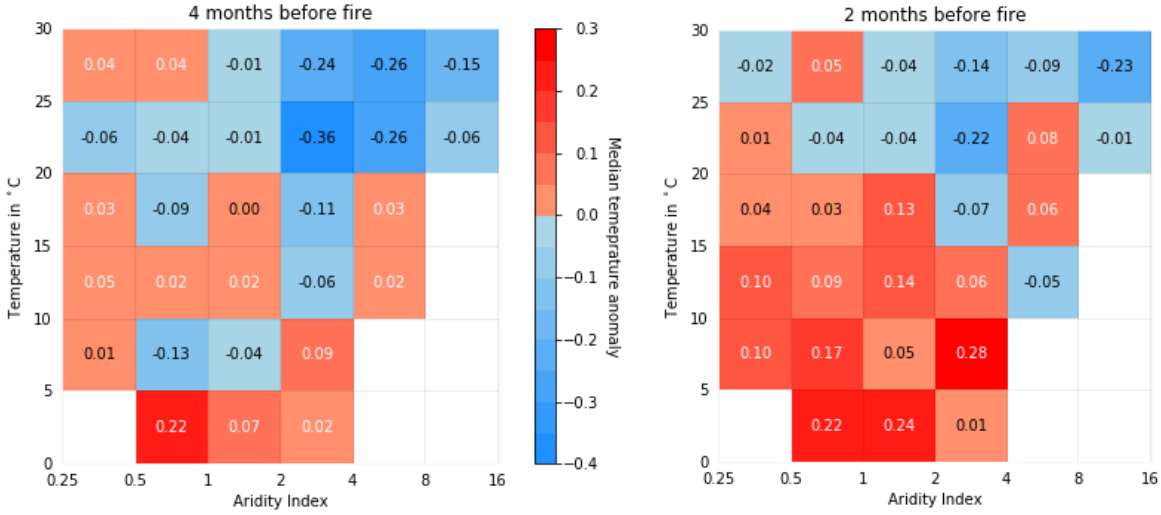

Figure 9: Median temperature anomaly of each regime. Left: four months before the month with the peak burned area; right: two months before the month with the peak burned area. The two heatmaps share the same color bar. Empty bins denote that the regime is left out due to its low number of grid cells with valid data (<100).

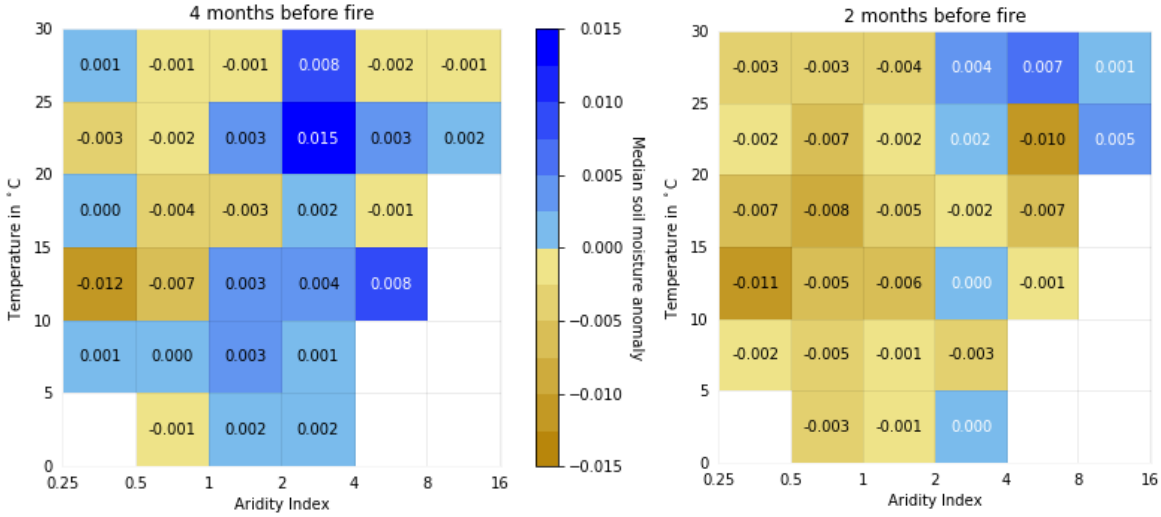

Figure 10: Median soil moisture anomaly of each regime. Left: four months before the month with the peak burned area; right: two months before the month with the peak burned area. The two heatmaps share the same color bar. Empty bins denote that the regime is left out due to its low number of grid cells with valid data (<100).

3.4 Post-fire recovery

Figure 11 shows the recovery time after the month with the peak burned area. The regimes have recovery time only when the median anomaly experiences a transition across the zero line (from negative to positive within eight months after the fire). In the arid regimes (AI > 4) exists considerable data gap.

The recovery time for NDVI shows no clear pattern across different climate regimes (Figure 11, left); in general, most regimes need two to four months for NDVI to return to the normal status. The similar amount of time applies to soil moisture recovery (Figure 11,

right). In the arid regimes (AI > 4) with moderate temperatures (10-20 °C), nearly half a year are needed to replenish the soil moisture deficit after the burn.

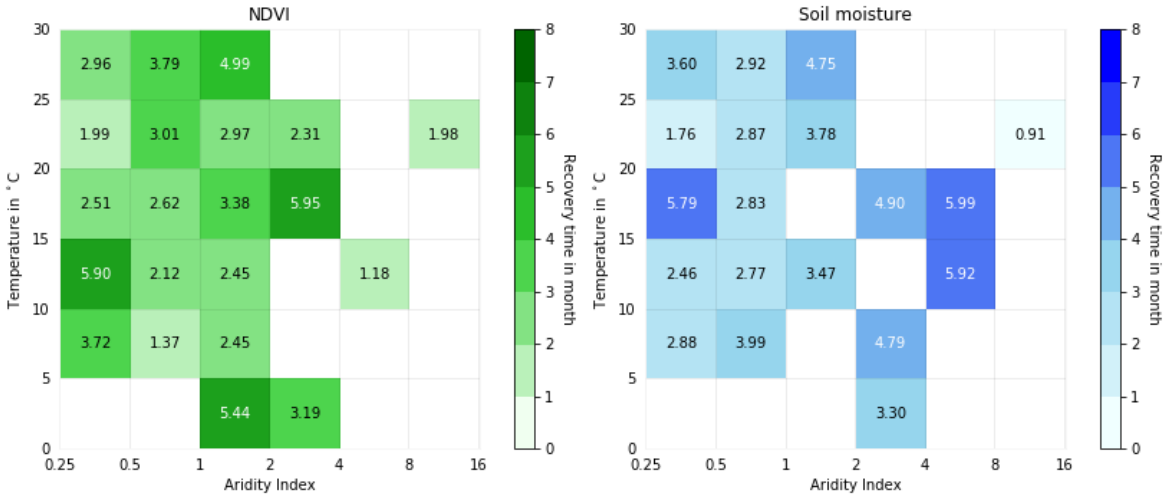

Figure 11: Recovery time in month within eight months after the month with the peak burned area for NDVI (left) and soil moisture (right). Empty bins denote that the regime is left out due to its low number of grid cells with positive burned area (<100) or lack of valid data despite a high number of grid cells with positive burned area.

4 Discussion

4.1 Comparison

Fires are not restricted to some certain regions or ecosystems and have considerable spatial and temporal variability. Under a warmer climate (IPCC, 2013), an increase is expected in burned area, fire weather severity, fire season length, number of ignitions with spatial and temporal variation (Flannigan et al., 2006).

Globally, fire happens most frequently within the aridity index range of 1 to 2. In wetter regions, it is more challenging to fulfill the physical conditions for fire ignition; in drier regions, fuel load would be scarce since vegetation would hardly thrive under the drought. Within this aridity range, fire occurrence along the temperature suggests a bimodal distribution. Not only do the hot regimes undergo frequent fire events, but fires in the cold regions also have a high frequency. A warmer and drier climate creates more fire-prone conditions (Flannigan et al., 2009; Forkel et al., 2019a). High temperature and dryness are associated with the increased burned area, probably because they are prerequisite for fuel dehydration; this statement holds up for a climate-limited fire regime instead of a fuel-limited one (Little et al., 2009). In fuel-limited regimes, increases in vegetation cover and density (the greening trends) result in burned area increase (Forkel et al., 2019b). However, according to model simulations, the increases in wetness and human population lead to burned area decrease, more than compensating the effect of temperature rise on increasing the burned area; the counteraction has its controls at regional scales (Forkel et al., 2019b).

Why the lowest frequency of fire occurrence (Burn Ratio) is observed in the moderate regime rather than the cold one under the same aridity might be explained by fire management. These regimes are denser-populated, and when people are accustomed to fire occurrence, they tend to be better adapted to tackle the fire with proper strategies such as the cultivation of less fire-prone vegetation or rapid suppression after fire ignitions.

Another possibility can be assorted fire types depending on the fuel types in different climate regimes. For example, the crown fire has a higher frequency in regions where more severe droughts and young plant stand prevail (Turner & Romme, 1994). Previous studies supported that in boreal forests, land cover plays a less critical role than in the Mediterranean regions where certain vegetation types are selectively burned (Moreira et al., 2011). Though Flannigan et al. (2016) corroborated that a wide range of good-adapted species in the boreal forest can thrive in a post-fire environment, post-fire plant communities or even future disturbance can be subject to long-term impacts by spatio-temporal variability of severity during one fire event (Ryan, 2002).

The temporal evolution of the burned area shows the most massive burning in the arid and hot regimes. It is thus reasonable to identify high temperatures as a crucial driving force

for fire severity. There is a fuel accumulation phase (featured by positive NDVI anomalies) prior to the fire outbreak and the consuming phase (positive anomalies turn negative) during the fire. The similar case applies to soil moisture anomalies during the pre-fire months, as moisture surplus promotes vegetation growth, which indirectly increases the fuel supply for later burning. Littell et al. (2009) confirmed that positive moisture anomalies lead to non-linear increases in the burned area by producing large continuous areas of fine fuel.

However, as time draws nearer until around two months before the fire, soil moisture is gradually depleted by higher temperatures or other factors. It is illustrated explicitly by the heatmaps of the pre-fire soil moisture anomaly. Such dry conditions may increase the vulnerability of vegetation to fire. For instance, Littell et al. (2009) suggested that warmer pre-fire conditions possibly increase burned area by facilitating plant growth in a warmer and wetter condition (the plants get exposed to more energy and moisture mainly originates from snowmelt); on the other hand, it can also eliminate carryover of soil moisture, hence limit fuel production, resulting in burned area decrease. The same authors inferred that moist conditions prior to the fire season are more crucial than high temperatures and drought in arid ecoregions. Moisture in the pre-fire seasons significantly influences the fire size, namely: small fires are more likely to occur when the condition is wet, large fires when it is dry (Krueger et al., 2015; Jensen et al., 2018). Even the surface soil moisture in the growing season has recovered from persistent droughts, the risk of fire outburst can still be high (Krueger et al., 2015). The same authors also stated that to fuel moisture, plant phenology likely matters more than soil moisture. Low moisture on foliage or fuel surface tends to facilitate fire spread (Swetnam & Betancourt, 1998).

Satellite-derived data indicate significant sensitivity of burned area to climate variables, vegetation properties, and socio-economic variables (Forkel et al., 2019a). Regimes with cold and wet conditions and those with hot and dry conditions are presumably both sensitive to temperature increase under the hint of the diagonal distribution on the corresponding heatmap. For the variable NDVI, its pre-fire anomalies across different climate regimes merely indicate a weak signal, which emphasizes the climate-dependency of interactions between vegetation and fire.

After the fire, the vegetation across different climate regimes needs different time to recover. Previous studies have reported that the post-fire vegetation recovery is highly dependent on fire intensity/interval, vegetation type, climate and topography (Bright et al., 2019). The apparent relationship between recovery time and climate is hard to establish within this study. However, the cold-wet, as well as the hot-arid regimes, seem more vulnerable to anomalies than other regimes.

4.2 Limitations

The fire data used here reported an underestimation of the burned area during 2001 and 2002 owing to the availability of the satellite Terra (Lizundia-Loiola et al., 2018). The extraction of burned area concerning this period might bring uncertainty. Although the employed burned area dataset has a remarkable spatial resolution, information of fire occurrence (such as the number or intensity of the fire) is unknown. Even though one only selects the largest fire event (identified by the largest burned area) throughout the 16 years in each grid cell, the extent of fire intensity is not intercomparable, since one large fire in one grid cell might be medium or even small in another grid cell. The more convincing approach would be to categorize fires according to their magnitude based on the size of the burned area. Besides, this dataset cannot distinguish between burned area caused by wildfire or human-ignited burning. A better indicator of ecological consequences of a fire could be fire severity, which is presumably better than burned area at capturing the effects of climate (Littell et al., 2009).

Being a proxy of vegetation activity, NDVI provides no information on vegetation composition or structure. However, vegetation composition could be essential in fire dynamics. For example, the abundance of *Pinus sylvestris* plays a critical role in forest fires in temperate climate zones (Adámek et al., 2015); in the Western US, burned area is predominantly influenced by changing fuel structure and composition (Little et al., 2009).

Another factor is that albeit the measure of greenness is chosen, it is less green plants that are more flammable. Senescent vegetation tends to turn yellow or brown. While the fuel is loading, the condition cannot be accurately reflected by NDVI. Biases might also come into being when surface fires are shadowed by the thick canopy (e.g., in the Amazon rainforest) - this burned area would not be detected by satellite instruments or at least largely underestimated.

For soil moisture, the spatial resolution of the data can be critical. As is generally acknowledged, even within a small area in the same field, the soil moisture is heterogeneous to a great extent (Seneviratne et al., 2010). The behaviors of median soil moisture anomalies in this study do not necessarily represent the actual moist status of the soil at the location of the fire. A clear relationship between pre-season soil moisture and fire occurrence might not exist, or other factors have masked it; however, across various land cover types, they can be strongly negative correlated (Jensen et al., 2018). In addition, it is sometimes impractical to categorize wildfire by one specific vegetation class; as Krueger et al. (2015) pointed out, large fires burn across various types of land cover.

Furthermore, NDVI and soil moisture are not independent of each other because NDVI is considered to change according to vegetation's interaction with soil moisture (Tucker, 1979). The performance of soil moisture datasets of remote-sensing source also varies depending on vegetation density (Liu et al., 2012).

5 Conclusion and outlook

In this thesis, the author mapped the fire occurrence distribution over the globe and examined the fire-vegetation-soil moisture interactions across different climate regimes. It is found that the fire has the highest frequency under the temperate aridity (aridity index range of 1 to 2). In the hot and arid regimes, more area tends to be burned during the fire. There is more burning in the cold regimes than in temperate ones. The temporal evolutions of anomalies of NDVI, temperature and soil moisture emit signals of fire occurrence. The pre-fire anomalies and post-fire recovery demonstrate the complexity of climate-fire interactions.

It is unfeasible to establish an absolute dichotomy between "moisture-limited" and "energy-limited" fire regime at the scale of ecoregions owing to the complexity which vegetation brings to the climate-fire relationship; evidence shows that there are fire regimes controlled by both fuel and climate because of the diversity of the responsible vegetation (Littell et al., 2009). In this sense, the impacts of plant functional types on fires merit further investigation. Future research should also address the effects of long-term and successional changes of vegetation composition and structure on burned area (Balshi et al., 2009).

The consequences of climate change on fire should be investigated with a consideration of locality (e.g., geographical division, climate division and ecosystem division). To date, only a few studies quantified the potential changes in fire regimes due to the climate (Flannigan et al., 2009). Apart from the spatial variability, temporal aspects (seasonal and inter-annual variations) could also be of great interest to studies on fire. Moreover, one can consider the influence of wind, soil texture and anthropogenic intervention.

Bibliography

Adámek, M., Bobek, P., Hadincová, V., Wild, J., and Kopecký, M.: Forest fires within a temperate landscape: A decadal and millennial perspective from a sandstone region in Central Europe, Forest Ecology and Management, 336, 81–90, https://doi.org/10.1016/j.foreco.2014.10.014, 2015.

Allen, R. G., Pereira, L. S., Raes, D., and Smith, M.: Crop evapotranspiration: Guidelines for computing crop water requirements: Paper no. 56. FAO, 1998.

Balshi, M. S., McGuire, A. D., Duffy, P., Flannigan, M., Walsh, J., and Melillo, J.: Assessing the response of area burned to changing climate in western boreal North America using a Multivariate Adaptive Regression Splines (MARS) approach, Global Change Biology, 15, 578–600, https://doi.org/10.1111/j.1365-2486.2008.01679.x, 2009.

Bright, B. C., Hudak, A. T., Kennedy, R. E., Braaten, J. d., and Henareh Khalyani, A.: Examining post-fire vegetation recovery with Landsat time series analysis in three western North American forest types, Fire Ecology, 15, 11 770, https://doi.org/10.1186/s42408-018-0021-9, 2019.

Budyko, M. I.: Climate and Life, Academic Press, London, 1974.

Burapapol, K. and Nagasawa, R.: Mapping Soil Moisture as an Indicator of Wildfire Risk Using Landsat 8 Images in Sri Lanna National Park, Northern Thailand, Journal of Agricultural Science, 8, 107, https://doi.org/10.5539/jas.v8n10p107, 2016.

Chuvieco, E., Yue, C., Heil, A., Mouillot, F., Alonso-Canas, I., Padilla, M., Pereira, J. M., Oom, D., and Tansey, K.: A new global burned area product for climate assessment of fire impacts, Global Ecology and Biogeography, 25, 619–629, https://doi.org/10.1111/geb.12440, 2016.

Copernicus Climate Change Service: ERA5: Fifth generation of ECMWF atmospheric reanalyses of the global climate., URL `https://cds.climate.copernicus.eu/cdsapp#!/home`, 2017.

Flannigan, M. D. and Wotton, B. M.: Climate, weather and area burned, in: Forest Fires: Behavior & Ecological Effects, edited by Johnson, E. A. and Miyanishi, K., pp. 335–357, Academic Press, New York, 2001.

Flannigan, M. D., Logan, K. A., Amiro, B. D., Skinner, W. R., and Stocks, B. J.: Future area burned in Canada, Climatic Change, 72, 1–16, https://doi.org/10.1007/s10584-005-5935-y, 2005.

Flannigan, M. D., Amiro, B. D., Logan, K. A., Stocks, B. J., and Wotton, B. M.: Forest Fires and Climate Change in the 21ST Century, Mitigation and Adaptation Strategies for Global Change, 11, 847–859, https://doi.org/10.1007/s11027-005-9020-7, 2006.

Flannigan, M. D., Stocks, B. J., Turetsky, M., and Wotton, B. M.: Impacts of climate change on fire activity and fire management in the circumboreal forest, Global Change Biology, 15, 549–560, https://doi.org/10.1111/j.1365-2486.2008.01660.x, 2009.

Flannigan, M. D., Wotton, B. M., Marshall, G. A., de Groot, W. J., Johnston, J., Jurko, N., and Cantin, A. S.: Fuel moisture sensitivity to temperature and precipitation: climate change implications, Climatic Change, 134, 59–71, https://doi.org/10.1007/s10584-015-1521-0, 2016.

Forkel, M., Dorigo, W., Lasslop, G., Teubner, I., Chuvieco, E., and Thonicke, K.: A data-driven approach to identify controls on global fire activity from satellite and climate observations (SOFIA V1), Geoscientific Model Development, 10, 4443–4476, https://doi.org/10.5194/gmd-10-4443-2017, 2017.

Forkel, M., Andela, N., Harrison, S. P., Lasslop, G., van Marle, M., Chuvieco, E., Dorigo, W., Forrest, M., Hantson, S., Heil, A., Li, F., Melton, J., Sitch, S., Yue, C., and Arneth, A.: Emergent relationships with respect to burned area in global satellite observations and fire-enabled vegetation models, Biogeosciences, 16, 57–76, https://doi.org/10.5194/bg-16-57-2019, 2019a.

Forkel, M., Dorigo, W., Lasslop, G., Chuvieco, E., Hantson, S., Heil, A., Teubner, I., Thonicke, K., and Harrison, S. P.: Recent global and regional trends in burned area and their compensating environmental controls, Environmental Research Communications, 1, 051 005, https://doi.org/10.1088/2515-7620/ab25d2, 2019b.

Giglio, L., Randerson, J. T., and van der Werf, G. R.: Analysis of daily, monthly, and annual burned area using the fourth-generation global fire emissions database (GFED4), Journal of Geophysical Research: Biogeosciences, 118, 317–328, https://doi.org/10.1002/jgrg.20042, 2013.

Hersbach, H. and Dee, D.: ERA5 reanalysis is in production, ECMWF Newsletter No.147, 7, 2016.

IPCC: Climate change 2013: The physical science basis : Working Group I contribution to the Fifth assessment report of the Intergovernmental Panel on Climate Change: [Stocker, T.F., D. Qin, G.-K. Plattner, M. Tignor, S.K. Allen, J. Boschung, A. Nauels, Y. Xia, V. Bex and P.M. Midgley (eds.)], Cambridge University Press, New York, 2013.

Jensen, D., Reager, J. T., Zajic, B., Rousseau, N., Rodell, M., and Hinkley, E.: The sensitivity of US wildfire occurrence to pre-season soil moisture conditions across ecosystems, Environmental Research Letters, 13, 014 021, https://doi.org/10.1088/1748-9326/aa9853, 2018.

Krueger, E. S., Ochsner, T. E., Engle, D. M., Carlson, J. D., Twidwell, D., and Fuhlendorf, S. D.: Soil Moisture Affects Growing-Season Wildfire Size in the Southern Great Plains, Soil Science Society of America Journal, 79, 1567, https://doi.org/10.2136/sssaj2015.01.0041, 2015.

Littell, J. S., Mckenzie, D., Peterson, D. L., and Westerling, A. L.: Climate and wildfire area burned in western U.S. ecoprovinces, 1916-2003, Ecological Applications, 19, 1003–1021, https://doi.org/10.1890/07-1183.1, 2009.

Liu, Y. Y., Dorigo, W. A., Parinussa, R. M., de Jeu, R., Wagner, W., McCabe, M. F., Evans, J. P., and van Dijk, A.: Trend-preserving blending of passive and active microwave soil moisture retrievals, Remote Sensing of Environment, 123, 280–297, https://doi.org/10.1016/j.rse.2012.03.014, 2012.

Lizundia-Loiola J., Pettinari M.L., Chuvieco E.: ESA CCI ECV Fire Disturbance: D3.3.3 Product User Guide - MODIS, version 1.2., 22.10.2018.

Moreira, F., Viedma, O., Arianoutsou, M., Curt, T., Koutsias, N., Rigolot, E., Barbati, A., Corona, P., Vaz, P., Xanthopoulos, G., Mouillot, F., and Bilgili, E.: Landscape - wildfire interactions in southern Europe: Implications for landscape management, Journal of Environmental Management, 92, 2389–2402, https://doi.org/10.1016/j.jenvman.2011.06.028, 2011.

Rouse, J. W., Haas, H. R., Deering, D. W., Schell, J. A., and Harlan, J. C.: Monitoring the vernal advancement and retrogradation (green wave effect) of natural vegetation, URL http://ntrs.nasa.gov/archive/nasa/casi.ntrs.nasa.gov/19740004927.pdf, 1974.

Ryan, K. C.: Dynamic interactions between forest structure and fire behavior in boreal ecosystems, Silva Fennica, 36, 13–39, 2002.

Schulzweida, U.: CDO User Guide (Version 1.9.6), URL http://doi.org/10.5281/zenodo.2558193, 2019.

Seneviratne, S. I., Corti, T., Davin, E. L., Hirschi, M., Jaeger, E. B., Lehner, I., Orlowsky, B., and Teuling, A. J.: Investigating soil moisture-climate interactions in a changing climate: A review, Earth-Science Reviews, 99, 125–161, https://doi.org/10.1016/j.earscirev.2010.02.004, 2010.

Swetnam, T. W. and Betancourt, J. L.: Mesoscale Disturbance and Ecological Response to Decadal Climatic Variability in the American Southwest, Journal of Climate, 11, 3128–3147, https://doi.org/10.1175/1520-0442(1998)011<3128:MDAERT>2.0.CO;2, 1998.

Tucker, C. J.: Red and photographic infrared linear combinations for monitoring vegetation, Remote Sensing of Environment, 8, 127–150, https://doi.org/10.1016/0034-4257(79)90013-0, 1979.

Turner, M. G. and Romme, W. H.: Landscape dynamics in crown fire ecosystems, Landscape Ecology, 9, 59–77, https://doi.org/10.1007/BF00135079, 1994.

Vermote, E., Justice, C., Csiszar, I., Eidenshink, J., Myneni, R., Baret, F., Masuoka, E., Wolfe, R., Claverie, M., and NOAA CDR Program: NOAA Climate Data Record (CDR) of Normalized Difference Vegetation Index (NDVI), Version 4, https://doi.org/10.7289/V5PZ56R6, 2014.

Youssouf, H., Liousse, C., Roblou, L., Assamoi, E. M., Salonen, R. O., Maesano, C., Banerjee, S., and Annesi-Maesano, I.: Quantifying wildfires exposure for investigating health-related effects, Atmospheric Environment, 97, 239–251, https://doi.org/10.1016/j.atmosenv.2014.07.041, 2014.